Acta Mech 198, 65–86 (2008)
DOI 10.1007/s00707-007-0517-x
Printed in The Netherlands

Acta Mechanica

Pattern instability of functionally graded and layered elastic films under van der Waals forces

X. Wang[1], L. J. Sudak[2], E. Pan[1]

[1] Department of Civil Engineering and Department of Applied Mathematics, University of Akron, Akron, OH, USA
[2] Department of Mechanical and Manufacturing Engineering, University of Calgary, Calgary, Canada

Received 17 April 2007; Accepted 27 September 2007; Published online 25 January 2008

Summary. This paper investigates surface instability of a functionally graded and layered elastic film interacting with another flat rigid body [or interacting with another functionally graded and layered elastic film (or simply-supported elastic plate)] through surface van der Waals forces under plane strain conditions. The shear modulus in each functionally graded layer is assumed to be exponentially varied in the thickness direction. A homogeneous elastic layer, which is the focus of this research, can be considered as a special case of the functionally graded layer by taking the magnitude of the gradient parameter to be very small. The solution for any functionally graded layer is obtained in terms of the pseudo-Stroh formalism; then the solution for the multilayered system is derived based on the transfer-matrix method. As a result the displacement and traction vectors at the top surface of the layered film (or plate) can be expressed in terms of those at the bottom surface of the layered film (or plate). We can thus obtain simple relationships between the surface normal traction and surface deflection. Expressions for the interaction coefficient as a function of the wave number of the instability mode are therefore obtained. The critical value of the interaction coefficient for surface instability and the associated instability mode can be determined easily by identifying the minimum of the interaction coefficient. An advantage of the present method lies in that it is very convenient to address a film (or a plate) with an arbitrary number of layers. The correctness of the present approach is verified by comparison with known results. The results show that it is possible to find N distinct surface instability modes for an N-layered elastic film interacting with another flat rigid body; and that it is also possible to find that there are at most N_1+N_2 distinct surface instability modes for an N_1-layered elastic film interacting with another N_2-layered elastic film. When a multilayered elastic film interacts with a simply-supported multilayered elastic plate, the film-plate system will exhibit the instability mode of the film or that of the plate depending on the stability strength of the plate versus that of the film.

1 Introduction

Surface instability of elastic thin films under an external field, such as van der Waals interactions or an electrostatic field, has been a topic of intensive research [1]–[11]. Monch and Herminghaus [1] and Shenoy and Sharma [2], [3] studied the surface instability of a rubber elastic layer bonded to a

Correspondence: Xu Wang, Department of Civil Engineering and Department of Applied Mathematics, University of Akron, Akron, OH 44325-3905, USA
e-mail: xuwang@uakron.edu

rigid substrate and attracted by a rigid contactor through van der Waals forces. It is found that the originally flat surface of the elastic film becomes wavy when the distance between the two surfaces is so small that the interaction exceeds a critical value. In addition, the fundamental surface instability mode of an elastic layer on a rigid substrate, attracted by a rigid flat surface, is determined by the thickness of the elastic layer, and is independent of the nature and magnitude of the interaction and elastic modulus of the film. Ru [4] investigated the surface instability of two mutually attracting films due to van der Waals forces by using an approximate method, which reduces the original two-dimensional problem of an elastic film to a one-dimensional surface problem. It is observed that two distinct metastable instability modes can emerge as a result of the incompatibility of the individual fundamental modes of the two elastic films with unequal thickness. Ru [5] also addressed the surface instability of an elastic thin film on a rigid substrate interacting with a suspended elastic plate through van der Waals forces by employing the same approximate method. He observed [5] that (1) when the stability strength of the plate is lower than the film, the interaction coefficient is an increasing function of the wave number, and then the film-plate system exhibits a long-wave instability mode of the suspended plate; (2) otherwise, the interaction coefficient admits an interval local minimum representing the short-wave modes of the film. Then the critical value and instability mode of the film-plate system are determined by the internal local minimum for shorter plates, or by the long-wave mode of the plate for longer plates. Most recently, Yoon et al. [6] studied the surface instability of a bilayer elastic film interacting with another rigid body through van der Waals forces by means of the approximate method used in [4] and [5]. They found that a bilayer elastic film can have two distinct surface instability modes when the top layer is more compliant and much thinner than the bottom layer. Huang et al. [7] studied the surface instability of an elastic film interacting with a rigid body through van der Waals forces by means of a three-dimensional approach. The surface instability of a semi-infinite elastic body (as in contrast to a film with finite thickness) under surface van der Waals forces has also been studied [8]–[11].

In this research, we investigate three typical cases of practical importance under plane strain conditions: (1) surface instability of a functionally graded and layered elastic film interacting with another flat rigid body through van der Waals forces; (2) surface instability of two mutually attracting functionally graded and layered elastic films due to van der Waals forces; (3) surface instability of a functionally graded and layered elastic film interacting with another simply-supported functionally graded and layered elastic plate through van der Waals forces. The shear modulus in each functionally graded layer is assumed to be exponentially varied in the thickness direction. It is found that the pseudo-Stroh formalism and the transfer-matrix method, which have been employed in the investigation of simply-supported multilayered rectangular plates made up of functionally graded materials (FGMs) [12], can also be conveniently applied to investigate the surface instability of FGM layered films. The solution for any FGM layer is obtained in terms of the pseudo-Stroh formalism; then the solution for the multilayered system is derived based on the transfer-matrix method. As a result the displacement and traction vectors at the top surface of the layered film (or plate) can be expressed in terms of those at the bottom surface of the layered film (or plate). Simple relationships between the surface normal traction and surface deflection can thus be obtained. One advantage of the present approach lies in that it can be employed to address the instability behavior of multilayered films (or plates) with arbitrary number of layers. Due to the fact that the focus of this research is on the instability of multilayered films made of *homogeneous* materials, then the magnitudes of the gradient parameters are taken to be very small during the calculations. It shall be mentioned that the pseudo-Stroh formalism for FGM is invalid for homogeneous material since the homogeneous material belongs to the mathematically degenerate material in which there are multiple identical eigenvalues and only one independent eigenvector associated with the identical eigenvalues exists. In Sect. 2, the relationships between the surface deflection and surface normal stress are derived for an FGM and layered elastic film and a plate. Expressions for the interaction coefficient as a function of the wave number of the instability mode for the three cases are obtained in Sects. 3–5. Detailed numerical results and discussions are presented in Sect. 6.

2 Surface deflection and surface normal stress relationship for an FGM layered film and an FGM layered plate

Let us first consider the plane strain deformation of an elastic film with thickness H fixed on a rigid substrate, as shown in Fig. 1. A Cartesian coordinate system (x_1, x_2) is established in such a way that the film-substrate interface is at $x_2 = 0$, while the top surface of the film is at $x_2 = H$. The elastic film is composed of N FGM layers, and layer k is bounded by its lower interface (or surface) at $x_2 = z_k$ and upper interface (or surface) at $x_2 = z_{k+1}$ with its thickness $h_k = z_{k+1} - z_k$. The layers are numbered sequentially starting from the bottom layer, and apparently $H = \sum_{k=1}^{N} h_k$. Perfect bonding conditions between two adjacent elastic layers are assumed in this research. The shear modulus within each FGM layer is exponentially varied along the x_2-direction, while Poisson's ratio is kept constant within the layer.

In a certain FGM layer, the linear constitutive equations are given by

$$\begin{aligned}\sigma_{11} &= \frac{2\mu(x_2)(1-\nu)}{1-2\nu}\varepsilon_{11} + \frac{2\mu(x_2)\nu}{1-2\nu}\varepsilon_{22},\\ \sigma_{22} &= \frac{2\mu(x_2)\nu}{1-2\nu}\varepsilon_{11} + \frac{2\mu(x_2)(1-\nu)}{1-2\nu}\varepsilon_{22},\\ \sigma_{12} &= \mu(x_2)\gamma_{12},\end{aligned} \tag{1}$$

where $\mu(x_2)$ and ν are shear modulus and Poisson's ratio, respectively. In this investigation, the shear modulus $\mu(x_2)$ obeys the following form:

$$\mu(x_2) = \mu_0 \exp(\beta x_2), \tag{2}$$

where μ_0 and β are material constants.

The displacement–strain relations are given by

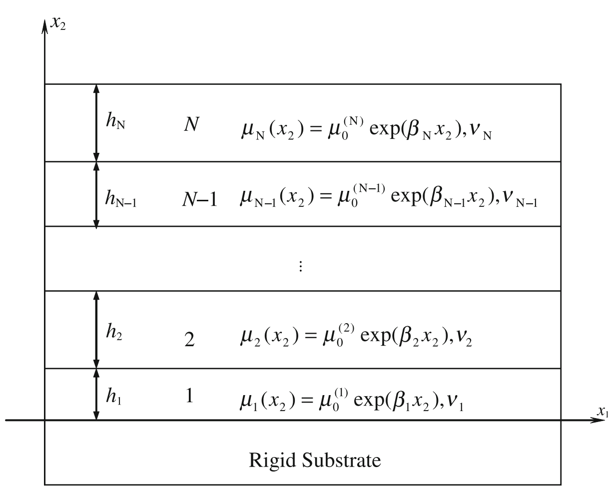

Fig. 1. An FGM multilayered elastic film on a rigid substrate

$$\varepsilon_{11} = \frac{\partial u_1}{\partial x_1}, \quad \varepsilon_{22} = \frac{\partial u_2}{\partial x_2}, \quad \gamma_{12} = \frac{\partial u_1}{\partial x_2} + \frac{\partial u_2}{\partial x_1}. \tag{3}$$

The equilibrium equations are given by

$$\begin{aligned} &\frac{\partial \sigma_{11}}{\partial x_1} + \frac{\partial \sigma_{12}}{\partial x_2} = 0, \\ &\frac{\partial \sigma_{12}}{\partial x_1} + \frac{\partial \sigma_{22}}{\partial x_2} = 0. \end{aligned} \tag{4}$$

Here the displacement vector can take the following form:

$$\mathbf{U} = \begin{bmatrix} u_1 \\ u_2 \end{bmatrix} = \exp(\lambda x_2) \begin{bmatrix} a_1 \sin(kx_1) \\ a_2 \cos(kx_1) \end{bmatrix}, \tag{5}$$

where k is the real positive wave number. Substitution of Eq. (5) into Eq. (2), and then the results into Eq. (1) yields the traction vector as

$$\mathbf{t} = \begin{bmatrix} \sigma_{12} \\ \sigma_{22} \end{bmatrix} = \exp\left[(\beta + \lambda)x_2\right] \begin{bmatrix} b_1 \sin(kx_1) \\ b_2 \cos(kx_1) \end{bmatrix}. \tag{6}$$

Now we introduce two 2×1 vectors $\mathbf{a}$ and $\mathbf{b}$,

$$\mathbf{a} = [\, a_1 \quad a_2 \,]^{\mathrm{T}}, \quad \mathbf{b} = [\, b_1 \quad b_2 \,]^{\mathrm{T}}, \tag{7}$$

then we can find that the vector $\mathbf{b}$ is related to $\mathbf{a}$ by

$$\mathbf{b} = (\mathbf{R}' + \lambda \mathbf{T})\mathbf{a} = -\frac{1}{\lambda}[\mathbf{Q} + \beta \mathbf{R}' + \lambda(\mathbf{R} + \beta \mathbf{T})]\mathbf{a}, \tag{8}$$

where $\mathbf{R}' = -\mathbf{R}^{\mathrm{T}}$, and the three 2×2 real matrices $\mathbf{T}$, $\mathbf{Q}$, $\mathbf{R}$ are defined by

$$\mathbf{T} = \mathbf{T}^{\mathrm{T}} = \mu_0 \begin{bmatrix} 1 & 0 \\ 0 & \frac{2(1-v)}{1-2v} \end{bmatrix}, \quad \mathbf{Q} = \mathbf{Q}^{\mathrm{T}} = -k^2 \mu_0 \begin{bmatrix} \frac{2(1-v)}{1-2v} & 0 \\ 0 & 1 \end{bmatrix}, \quad \mathbf{R} = k\mu_0 \begin{bmatrix} 0 & -\frac{2v}{1-2v} \\ 1 & 0 \end{bmatrix}. \tag{9}$$

Now inserting Eq. (5) into Eq. (2), then into Eq. (1), and finally into the equilibrium equations (4), we arrive at the following eigenrelations:

$$\left[\mathbf{Q} + \beta \mathbf{R}' + \lambda(\mathbf{R} + \mathbf{R}' + \beta \mathbf{T}) + \lambda^2 \mathbf{T}\right]\mathbf{a} = \mathbf{0}. \tag{10}$$

It can be easily verified that if λ is an eigenvalue of Eq. (10), then $-\beta - \lambda$ is also an eigenvalue of the eigenequation (10) [12]. Equation (10) can be recast into the following standard eigenrelations:

$$\mathbf{N} \begin{bmatrix} \mathbf{a} \\ \mathbf{b} \end{bmatrix} = \lambda \begin{bmatrix} \mathbf{a} \\ \mathbf{b} \end{bmatrix}, \tag{11}$$

where

$$\mathbf{N} = \begin{bmatrix} -\mathbf{T}^{-1}\mathbf{R}' & \mathbf{T}^{-1} \\ -\mathbf{Q} + \mathbf{R}\mathbf{T}^{-1}\mathbf{R}' & -\mathbf{R}\mathbf{T}^{-1} - \beta \mathbf{I} \end{bmatrix}. \tag{12}$$

We assume that the i-th ($i = 1,2$) and $(i+2)$-th eigenvalues of Eq. (11), denoted by λ_i and λ_{i+2}, satisfy the relation $\lambda_i + \lambda_{i+2} = -\beta$. Also, we distinguish the four eigenvectors of Eq. (11) by attaching a subscript to $\mathbf{a}$ and $\mathbf{b}$. Then the general solution for the displacement and traction vectors (of the x_2-dependent factor) can be concisely expressed as

$$\begin{bmatrix} \mathbf{U} \\ \mathbf{t} \end{bmatrix} = \begin{bmatrix} \mathbf{I} & \mathbf{0} \\ \mathbf{0} & \mathrm{e}^{\beta x_2}\mathbf{I} \end{bmatrix} \begin{bmatrix} \mathbf{A}_1 & \mathbf{A}_2 \\ \mathbf{B}_1 & \mathbf{B}_2 \end{bmatrix} \langle \mathrm{e}^{\lambda_\alpha x_2} \rangle \begin{bmatrix} \mathbf{K}_1 \\ \mathbf{K}_2 \end{bmatrix}, \tag{13}$$

where $\mathbf{K}_1$ and $\mathbf{K}_2$ are two 2×1 constant vectors to be determined, and

$$\begin{aligned} &\mathbf{A}_1 = [\,\mathbf{a}_1 \quad \mathbf{a}_2\,], \quad \mathbf{A}_2 = [\,\mathbf{a}_3 \quad \mathbf{a}_4\,], \\ &\mathbf{B}_1 = [\,\mathbf{b}_1 \quad \mathbf{b}_2\,], \quad \mathbf{B}_2 = [\,\mathbf{b}_3 \quad \mathbf{b}_4\,], \\ &\langle \mathrm{e}^{\lambda_\alpha x_2} \rangle = \mathrm{diag}\big[\,\mathrm{e}^{\lambda_1 x_2} \quad \mathrm{e}^{\lambda_2 x_2} \quad \mathrm{e}^{-(\beta+\lambda_1)x_2} \quad \mathrm{e}^{-(\beta+\lambda_2)x_2}\,\big]. \end{aligned} \tag{14}$$

The above formulations (11)–(13) can be termed the pseudo-Stroh formalism which has been adopted in the study of simply-supported FGM plates [12]. Here, we point out that the so-called pseudo-Stroh formalism, which is in a sense similar to (but not the same as) the Stroh formalism [13], [14] for two-dimensional deformations of anisotropic solids, was originally developed to investigate the simply-supported homogeneously orthotropic plates [15], and was later extended to address the simply-supported FGM plates [12], [16]. The validity of the simple pseudo-Stroh formalism is that all the eigenvalues must be *distinct* [12], [15], [16]. Should repeated roots occur for mathematically degenerate material such as the homogeneously isotropic material, a small perturbation technique [17] can still be conveniently employed to make all the eigenvalues distinct so that the simple and unified solution presented here can still be used.

The eigenvectors of Eq. (11) are actually the right ones. The left eigenvectors of Eq. (11) are found by solving the following eigenvalue problem:

$$\mathbf{N}^{\mathrm{T}}\boldsymbol{\eta} = s\boldsymbol{\eta}. \tag{15}$$

If λ and $[\mathbf{a}, \mathbf{b}]^{\mathrm{T}}$ are the eigenvalue and eigenvector of Eq. (11), then $s = -\beta - \lambda$ and $\boldsymbol{\eta} = [-\mathbf{b},\ \mathbf{a}]^{\mathrm{T}}$ are the corresponding solutions of Eq. (15). Since the left and right eigenvectors are orthogonal to each other, we then come to the following important orthogonal relationship [12], [15], [16]:

$$\begin{bmatrix} -\mathbf{B}_2^{\mathrm{T}} & \mathbf{A}_2^{\mathrm{T}} \\ \mathbf{B}_1^{\mathrm{T}} & -\mathbf{A}_1^{\mathrm{T}} \end{bmatrix} \begin{bmatrix} \mathbf{A}_1 & \mathbf{A}_2 \\ \mathbf{B}_1 & \mathbf{B}_2 \end{bmatrix} = \begin{bmatrix} \mathbf{I} & \mathbf{0} \\ \mathbf{0} & \mathbf{I} \end{bmatrix}. \tag{16}$$

Thus the orthogonal relationship Eq. (16) provides us with a simple way of inverting the eigenvector matrix, which is required in forming the transfer matrix.

In addition, the four eigenvalues of Eq. (11) can be explicitly given by

$$\lambda_1 = -\frac{\beta}{2} + \left[k^4 + \frac{\beta^2 k^2 (1+v)}{2(1-v)} + \frac{\beta^4}{16}\right]^{1/4} \exp\left(\frac{\mathrm{i}\theta}{2}\right), \quad \lambda_2 = \bar{\lambda}_1, \quad \lambda_3 = -\beta - \lambda_1, \quad \lambda_4 = -\beta - \bar{\lambda}_1, \tag{17}$$

where

$$\theta = \tan^{-1}\left(\frac{\beta k \sqrt{\frac{v}{1-v}}}{k^2 + \frac{\beta^2}{4}}\right). \tag{18}$$

It is found that when $\beta = 0$ for homogeneous material, multiple identical eigenvalues $\lambda_1 = \lambda_2 = k$, $\lambda_3 = \lambda_4 = -k$ will appear, but there is only one independent eigenvector associated with $\lambda_1 = \lambda_2 = k$ or $\lambda_3 = \lambda_4 = -k$. Thus the pseudo-Stroh formalism is not directly suitable for homogeneous material. When addressing homogeneous materials, we can adopt a small perturbation technique [17] by letting the magnitude of the gradient parameter β of the FGM film or plate to be very small with the obtained results sufficiently accurate with negligible error. In other words we can treat the homogeneous film or plate as *virtual* FGM film or plate with the magnitude of the gradient β very small but nonzero so that the pseudo-Stroh formalism presented here can still be utilized.

For a certain FGM elastic layer k with the lower surface at $x_2=z_k$ ($k=1,2,\ldots,N$), it follows from Eqs. (13) and (16) that $\mathbf{K}_1$ and $\mathbf{K}_2$ can be expressed in terms of displacement and traction vectors at the lower surface $x_2=z_k$ as

$$\begin{bmatrix}\mathbf{K}_1\\ \mathbf{K}_2\end{bmatrix}=\langle \mathrm{e}^{-s_\alpha z_k}\rangle\begin{bmatrix}-\mathbf{B}_2^{\mathrm{T}} & \mathbf{A}_2^{\mathrm{T}}\\ \mathbf{B}_1^{\mathrm{T}} & -\mathbf{A}_1^{\mathrm{T}}\end{bmatrix}\begin{bmatrix}\mathbf{I} & \mathbf{0}\\ \mathbf{0} & \mathrm{e}^{-lz_k}\mathbf{I}\end{bmatrix}\begin{bmatrix}\mathbf{U}\\ \mathbf{t}\end{bmatrix}_{z_k}. \tag{19}$$

Then the displacement and traction vectors at any position within this FGM layer are related to the displacement and traction vectors at the lower surface $x_2=z_k$ as follows:

$$\begin{bmatrix}\mathbf{U}\\ \mathbf{t}\end{bmatrix}=\mathbf{E}_k(x_2-z_k)\begin{bmatrix}\mathbf{U}\\ \mathbf{t}\end{bmatrix}_{z_k}, \tag{20}$$

where

$$\mathbf{E}_k(x)=\begin{bmatrix}\mathbf{I} & \mathbf{0}\\ \mathbf{0} & \mathrm{e}^{\beta(z_k+x)}\mathbf{I}\end{bmatrix}\begin{bmatrix}\mathbf{A}_1 & \mathbf{A}_2\\ \mathbf{B}_1 & \mathbf{B}_2\end{bmatrix}\langle \mathrm{e}^{s_\alpha x}\rangle\begin{bmatrix}-\mathbf{B}_2^{\mathrm{T}} & \mathbf{A}_2^{\mathrm{T}}\\ \mathbf{B}_1^{\mathrm{T}} & -\mathbf{A}_1^{\mathrm{T}}\end{bmatrix}\begin{bmatrix}\mathbf{I} & \mathbf{0}\\ \mathbf{0} & \mathrm{e}^{-\beta z_k}\mathbf{I}\end{bmatrix}, \tag{21}$$

is the transfer matrix of the FGM layer.

It follows from Eq. (20) that the solution at the upper surface $x_2=z_{k+1}$ of layer k is related to that at the lower surface $x_2=z_k$ of layer k through the following relation:

$$\begin{bmatrix}\mathbf{U}\\ \mathbf{t}\end{bmatrix}_{z_{k+1}}=\mathbf{E}_k(h_k)\begin{bmatrix}\mathbf{U}\\ \mathbf{t}\end{bmatrix}_{z_k}. \tag{22}$$

Consequently, the solution at the top surface $x_2=H$ of the film can be expressed by that at the bottom surface $x_2=0$ of the film as

$$\begin{bmatrix}\mathbf{U}\\ \mathbf{t}\end{bmatrix}_{H}=\mathbf{Y}\begin{bmatrix}\mathbf{U}\\ \mathbf{t}\end{bmatrix}_{0}, \tag{23}$$

where

$$\mathbf{Y}=\begin{bmatrix}Y_{11} & Y_{12} & Y_{13} & Y_{14}\\ Y_{21} & Y_{22} & Y_{23} & Y_{24}\\ Y_{31} & Y_{32} & Y_{33} & Y_{34}\\ Y_{41} & Y_{42} & Y_{43} & Y_{44}\end{bmatrix}=\mathbf{E}_N(h_N)\times\mathbf{E}_{N-1}(h_{N-1})\times\ldots\times\mathbf{E}_2(h_2)\times\mathbf{E}_1(h_1). \tag{24}$$

Due to the fact that the film is fixed on the substrate, i.e., $u_1(0)=u_2(0)=0$, and that $\sigma_{12}(H)=0$, then we can arrive at the following relationship between the surface deflection $u_2(H)$ and surface normal stress $\sigma_{22}(H)$ for a film as

$$\frac{\sigma_{22}(H)}{u_2(H)}=\frac{Y_{33}Y_{44}-Y_{34}Y_{43}}{Y_{24}Y_{33}-Y_{23}Y_{34}}. \tag{25}$$

The above derivations for an FGM layered elastic film can also be easily extended to the study of a simply-supported and FGM layered elastic plate, as shown in Fig. 2. The two sides $x_1=\pm L/2$ are simply-supported, i.e., $u_2=\sigma_{11}=0$ at $x_1=\pm L/2$, and the traction-free conditions $\sigma_{12}=\sigma_{22}=0$ are imposed on the bottom surface $x_2=0$. The above derivations from Eqs. (1)–(24) are still valid by letting $k=(2n-1)\pi/L$, $n=1, 2, 3, \ldots$, so as to satisfy the simply-supported boundary conditions. The satisfaction of traction-free boundary conditions $\sigma_{12}(0)=\sigma_{22}(0)=0$ on the bottom surface $x_2=0$ and $\sigma_{12}(H)=0$ on the top surface $x_2=H$ yields

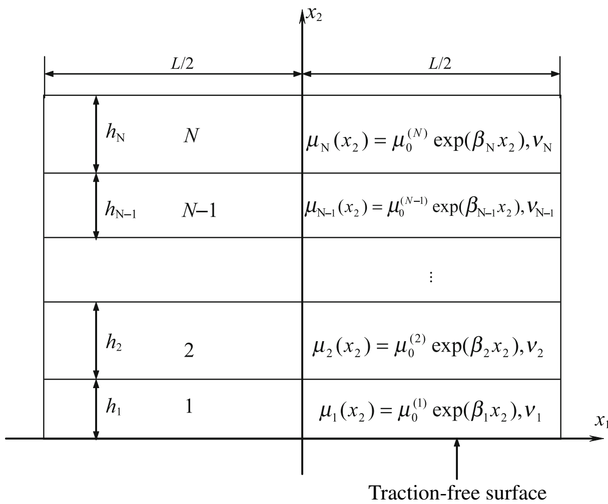

Fig. 2. A simply-supported and FGM multilayered elastic plate

the following relationship between the surface deflection $u_2(H)$ and surface normal stress $\sigma_{22}(H)$ for a plate as

$$\frac{\sigma_{22}(H)}{u_2(H)} = \frac{Y_{41}Y_{32} - Y_{42}Y_{31}}{Y_{21}Y_{32} - Y_{22}Y_{31}}. \tag{26}$$

3 A multilayered elastic film interacting with a flat rigid body

We now consider the surface instability of an N-layered elastic film with total thickness H interacting with a flat rigid body through surface van der Waals forces, as shown in Fig. 3. When two flat solid surfaces are brought into contact, van der Waals forces come into play if the gap between the two surfaces is very small (say, well below 100 nm, [5]). The surface conditions for the perturbed elastic film can be written as

$$\sigma_{22}(H) = Au_2(H), \tag{27}$$

where $A(>0)$ is the van der Waals interaction coefficient. Thus the surface interaction acts like a linear spring with a negative spring constant [4]. In the above expression, we have ignored the effect of the surface energy [2], [3].

Then it follows from Eqs. (25) and (27) that

$$A = \frac{Y_{33}Y_{44} - Y_{34}Y_{43}}{Y_{24}Y_{33} - Y_{23}Y_{34}}. \tag{28}$$

The critical value of the interaction coefficient A for the surface instability and the associated surface instability mode can be determined by finding the minimum of A given by Eq. (28) with respect to the variable k.

4 Two mutually attracting multilayered elastic films

The present formulation can also be easily applied to investigate the surface instability of two mutually attracting elastic films due to van der Waals forces. As illustrated in Fig. 4, we investigate an N_1-layered elastic film with a total thickness H_1 interacting with another N_2-layered elastic film with a total thickness H_2 through van der Waals forces. It follows from Eq. (25) that the relationship

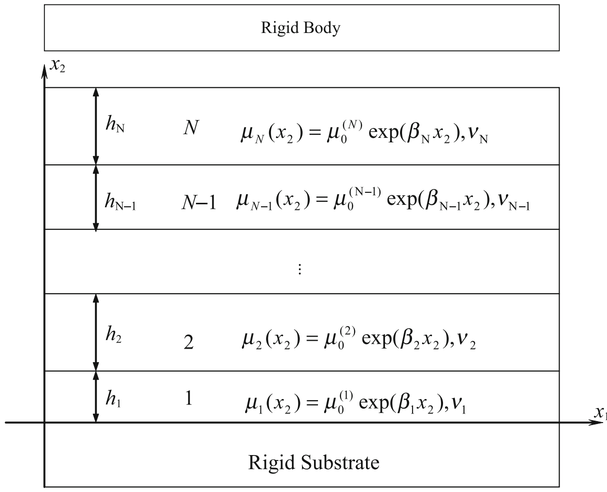

Fig. 3. Surface instability of an FGM multilayered elastic film interacting with a rigid body

between the (upward) surface deflection $u_2(H_1)$ and surface normal stress $\sigma_{22}(H_1)$ for the lower elastic film of thickness H_1 can be written as

$$\frac{\sigma_{22}(H_1)}{u_2(H_1)} = \frac{Y_{33}Y_{44} - Y_{34}Y_{43}}{Y_{24}Y_{33} - Y_{23}Y_{34}}, \tag{29}$$

while the relationship between the (downward) surface deflection $\tilde{u}_2(H_2)$ and surface normal stress $\tilde{\sigma}_{22}(H_2)$ for the upper elastic film of thickness H_2 can be written as

$$\frac{\tilde{\sigma}_{22}(H_2)}{\tilde{u}_2(H_2)} = \frac{\tilde{Y}_{33}\tilde{Y}_{44} - \tilde{Y}_{34}\tilde{Y}_{43}}{\tilde{Y}_{24}\tilde{Y}_{33} - \tilde{Y}_{23}\tilde{Y}_{34}}, \tag{30}$$

where '$\sim$' is added to the components to indicate that these components belong to the upper elastic film.

Meanwhile, the surface conditions for the two perturbed elastic films are given by

$$\sigma_{22}(H_1) = \tilde{\sigma}_{22}(H_2) = A[u_2(H_1) + \tilde{u}_2(H_2)], \tag{31}$$

where $A(>0)$ is again the van der Waals interaction coefficient.

Then it follows from Eqs. (29)–(31) that

$$A = \frac{1}{\frac{Y_{24}Y_{33} - Y_{23}Y_{34}}{Y_{33}Y_{44} - Y_{34}Y_{43}} + \frac{\tilde{Y}_{24}\tilde{Y}_{33} - \tilde{Y}_{23}\tilde{Y}_{34}}{\tilde{Y}_{33}\tilde{Y}_{44} - \tilde{Y}_{34}\tilde{Y}_{43}}}. \tag{32}$$

The critical value of the interaction coefficient A for the surface instability and the associated surface instability mode can be determined by finding the minimum of A given by Eq. (32) with respect to the variable k.

5 A multilayered elastic film interacting with a multilayered elastic plate

As illustrated in Fig. 5, we investigate an N_1-layered elastic film with a total thickness H_1 interacting with another simply-supported and N_2-layered elastic plate with a total thickness H_2 and length L through van der Waals forces. It follows from Eq. (25) that the relationship between the (upward) surface deflection $u_2(H_1)$ and surface normal stress $\sigma_{22}(H_1)$ for the lower elastic film of thickness H_1 can be written as

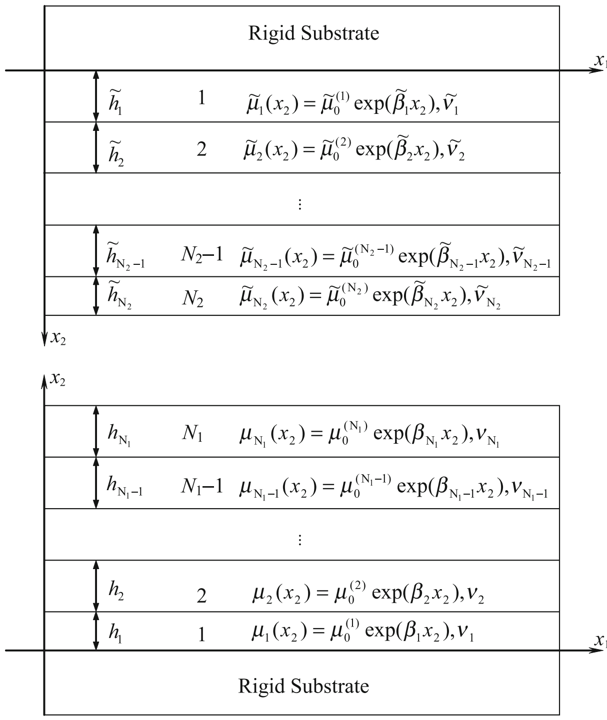

Fig. 4. Surface instability of two mutually attracting FGM multilayered elastic films

$$\frac{\sigma_{22}(H_1)}{u_2(H_1)} = \frac{Y_{33}Y_{44} - Y_{34}Y_{43}}{Y_{24}Y_{33} - Y_{23}Y_{34}}, \tag{33}$$

while it follows from Eq. (26) that the relationship between the (downward) surface deflection $\tilde{u}_2(H_2)$ and surface normal stress $\tilde{\sigma}_{22}(H_2)$ for the upper simply-supported elastic plate of thickness H_2 can be written as

$$\frac{\tilde{\sigma}_{22}(H_2)}{\tilde{u}_2(H_2)} = \frac{\tilde{Y}_{41}\tilde{Y}_{32} - \tilde{Y}_{42}\tilde{Y}_{31}}{\tilde{Y}_{21}\tilde{Y}_{32} - \tilde{Y}_{22}\tilde{Y}_{31}}, \tag{34}$$

where '$\sim$' is added to the components to indicate that these components belong to the upper elastic plate.

Meanwhile, the surface conditions for the perturbed film-plate system are given by

$$\sigma_{22}(H_1) = \tilde{\sigma}_{22}(H_2) = A[u_2(H_1) + \tilde{u}_2(H_2)], \tag{35}$$

where A(>0) is again the van der Waals interaction coefficient.

Then it follows from Eqs. (33)–(35) that

$$A = \frac{1}{\frac{Y_{24}Y_{33}-Y_{23}Y_{34}}{Y_{33}Y_{44}-Y_{34}Y_{43}} + \frac{\tilde{Y}_{21}\tilde{Y}_{32}-\tilde{Y}_{22}\tilde{Y}_{31}}{\tilde{Y}_{41}\tilde{Y}_{32}-\tilde{Y}_{42}\tilde{Y}_{31}}}. \tag{36}$$

The critical value of the interaction coefficient A for the surface instability and the associated surface instability mode can be determined by finding the minimum of A given by Eq. (36) with respect to the variable k under the constraint $k = (2n - 1)\pi/L$, $n = 1, 2, 3, \ldots$. In particular, the admissible values of k are bounded from below by the condition

$$k = (2n - 1)\pi/L \geq \pi/L. \tag{37}$$

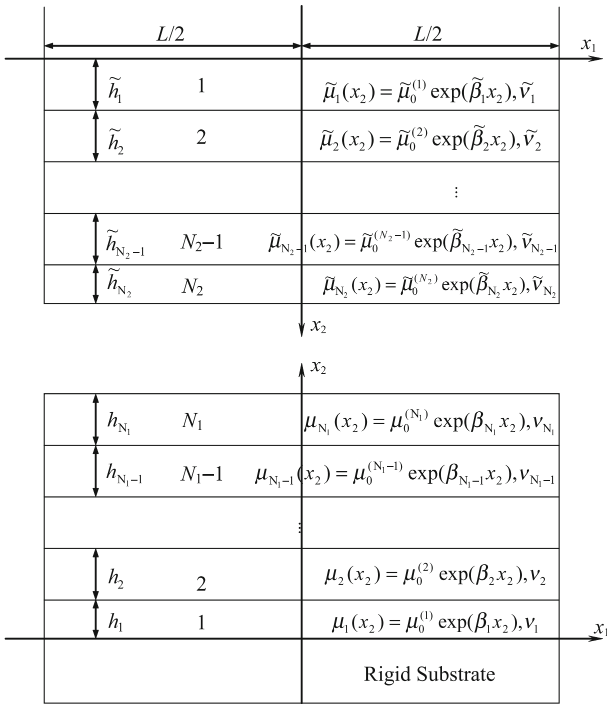

Fig. 5. Surface instability of an FGM multilayered film interacting with another simply-supported FGM layered elastic plate

6 Results and discussions

Due to the fact that the main goal of this research is not on the influence of the gradient parameter on the surface instability of the film (or the plate), then in the following calculations we only consider the case in which each layer of the film (or the plate) is homogeneous by letting the magnitude of the gradient parameter β be small enough. It is observed that all the results presented by Shenoy and Sharma [2], [3] for a single-layer elastic film interacting with a rigid body can be exactly recovered by using the present approach. Consequently, the correctness of the present approach is verified.

6.1 A multilayered elastic film interacting with another flat rigid body

We examine the surface instability of a multilayered elastic film interacting with another flat rigid body through van der Waals forces. The critical value of the interaction coefficient A for the surface instability is given by the minimum of Eq. (28). One main discovery of this investigation is that it is possible to find N local minima of Eq. (28), modes for an N-layered elastic film interacting with another flat rigid body. For example, for a three-layered film, if we choose $v_1=v_2=v_3=0.5$, μ_1:μ_2:$\mu_3=1$:0.1:0.01 and h_1 :h_2 :$h_3=1$:0.1:0.01, then there exist three local minima of Eq. (28) at $h_1\,k=2.03$, 16.47, 173 as shown in Fig. 6. Another example is for a four-layered film. If we choose $v_1=v_2=v_3=v_4=0.3$, μ_1:μ_2:μ_3:$\mu_4=1$:0.004:0.004^2:0.004^3 and h_1:h_2:h_3:$h_4=1$:1/9:1/81:1/729, then there exist four local minima of Eq. (28) at $h_1k=1.52$, 11.32, 78.6, 489 as shown in Fig. 7. In the following, we will discuss in more detail a three-layered film and a four-layered film interacting with a flat rigid body.

a. A three-layered elastic film interacting with a flat rigid body

We first consider the case in which the three layers are incompressible materials ($v_1 = v_2 = v_3 = 0.5$). All local minima of A as a function of $h_1 k$ are determined. In Figs. 8–12, the dimensionless wavelength $2\pi/[k(h_1 + h_2 + h_3)]$ and the dimensionless interaction coefficients $A(h_1/\mu_1 + h_2/\mu_2 + h_3/\mu_3)$, Ah_1/μ_1, Ah_2/μ_2, Ah_3/μ_3 at all local minima are plotted as a function of the shear modulus ratio $\mu_2/\mu_1 = \mu_3/\mu_2$. It is observed that:

- When $\mu_1 = \mu_2 = \mu_3$, the wavelength $2\pi/[k(h_1 + h_2 + h_3)]$ is 2.96 and the interaction coefficient $A(h_1/\mu_1 + h_2/\mu_2 + h_3/\mu_3)$ is 6.22 no matter what the thickness ratio $h_2/h_1 = h_3/h_2$ is. This result is in agreement with the fact that the elastic properties of the three layers are identical when $\mu_1 = \mu_2 = \mu_3$, and then they can be treated as a single layer with thickness $h = h_1 + h_2 + h_3$.
- When $\mu_2/\mu_1 = \mu_3/\mu_2 \leq 0.045$ and $h_2/h_1 = h_3/h_2 \geq 0.1$, Ah_3/μ_3 is very close to 6.22 (see Fig. 10), the critical value of the top elastic layer when the middle layer is treated as a rigid substrate. Meanwhile, $2\pi/[k(h_1 + h_2 + h_3)$] is about 0.0267, 0.228, 0.9879, 2.0518, 2.6701, for the thickness ratio $h_2/h_1 = h_3/h_2 = 0.1$, $1/3$, 1, 3, 10, all of which corresponding to $kh_3 = 2.12$, the wave number of the top layer when the middle layer is treated as a rigid substrate. This phenomenon is in agreement with the observation by Yoon et al. [6] for a bilayer elastic film.
- Three distinct surface instability modes exist for the three-layered elastic film when $h_2/h_1 = h_3/h_2 = 0.1$ and $0.054 \leq \mu_2/\mu_1 = \mu_3/\mu_2 \leq 0.15$. More specifically, for $h_2/h_1 = h_3/h_2 = 0.1$, the long-wave mode exists when $\mu_2/\mu_1 = \mu_3/\mu_2 \geq 0.054$; the medium-wave mode exists when $0.045 \leq \mu_2/\mu_1 = \mu_3\ /\mu_2 \leq 0.17$; the short-wave mode exists when $\mu_2/\mu_1 = \mu_3/\mu_2 \leq 0.15$. Ru [4] and Yoon et al. [6] have observed that double modes exist for two mutually attracting single-layer elastic films or for a bilayer elastic film interacting with a rigid body. Thus the present observation can be considered as an extension of the results of Ru [4] and Yoon et al. [6] to the more general multilayer case.

Next, we present the corresponding results in Figs. 13–17 for three compressible elastic layers with equal Poisson's ration $v_1 = v_2 = v_3 = 0.35$. The following can be observed:

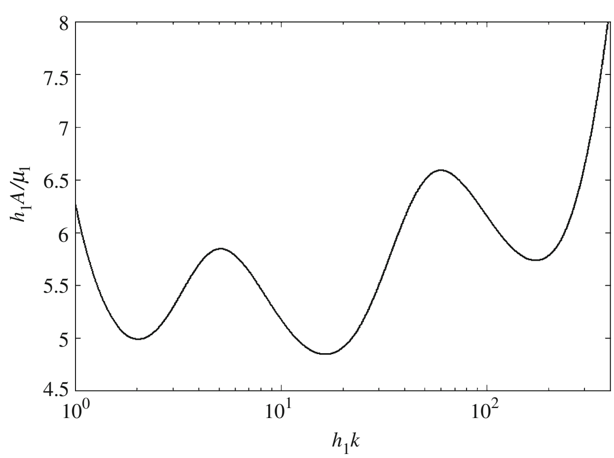

Fig. 6. The interaction coefficient Ah_1/μ_1 of a three-layered elastic film ($v_1 = v_2 = v_3 = 0.5$, μ_1:μ_2:$\mu_3 = 1$:0.1:0.01 and h_1:h_2:$h_3 = 1$:0.1:0.01) which, as a function h_1k, has three local minima

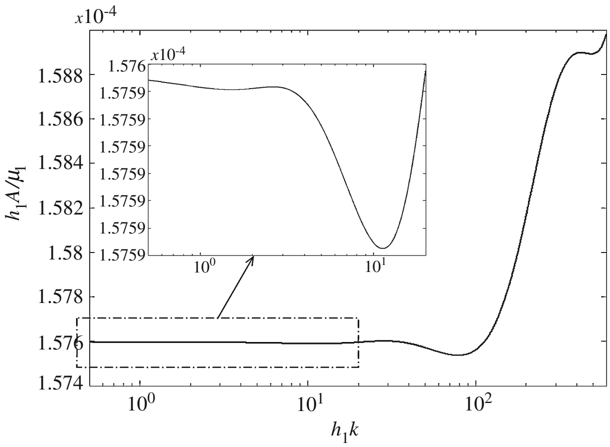

Fig. 7. The interaction coefficient Ah_1/μ_1 of a four-layered elastic film ($v_1 = v_2 = v_3 = v_4 = 0.3$, μ_1:μ_2:μ_3:$\mu_4 = 1$:0.004:0.004^2 :0.004^3 and h_1:h_2:h_3:$h_4 = 1$:1/9:1/81:1/729) which, as a function h_1k, has four local minima

- When $\mu_2/\mu_1 = \mu_3/\mu_2 \leq 0.0065$ and $h_2/h_1 = h_3/h_2 \geq 0.1$, Ah_3/μ_3 is very close to 3.94 (see Fig. 15), the critical value of the top elastic layer when the middle layer is treated as a rigid substrate.
- It is found from Fig. 17 that Ah_1/μ_1 is very close to 3.94, the critical value of the bottom elastic layer alone in the absence of the upper two elastic layers, when $0.1 \leq h_2/h_1 = h_3/h_2 \leq 10$ and the shear modulus ratio $\mu_2/\mu_1 = \mu_3/\mu_2$ is between 100 and 1,000. In other words, even though the upper two elastic layers are much stiffer than the bottom elastic layer, they can barely increase the strength of the bottom elastic layer against the surface instability.
- Three distinct surface instability modes exist for the three-layered elastic film when $h_2/h_1 = h_3/h_2 = 0.1$ and $0.0065 \leq \mu_2/\mu_1 = \mu_3/\mu_2 \leq 0.021$. More specifically, for $h_2/h_1 = h_3/h_2 = 0.1$, the long-wave mode exists when $\mu_2/\mu_1 = \mu_3/\mu_2 \geq 0.0065$; the medium-wave mode exists when $0.0045 \leq \mu_2/\mu_1 = \mu_3/\mu_2 \leq 0.024$; the short-wave mode exists when $\mu_2/\mu_1 = \mu_3/\mu_2 \leq 0.021$. This is similar to the incompressible case. In fact if $h_2/h_1 = h_3/h_2 = 0.1$, $\mu_2/\mu_1 = \mu_3/\mu_2$ and $v_1 = v_2 = v_3 = v$, our calculations show that it is possible to find triple modes when the Poisson's ratio satisfies the condition $0.283 \leq v \leq 0.5$.

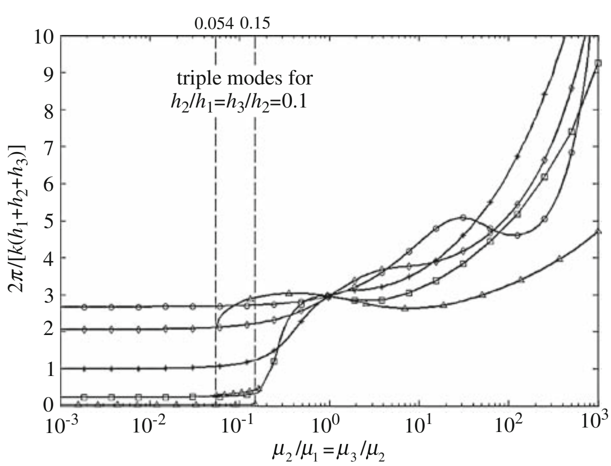

Fig. 8. Dimensionless wavelength $2\pi/[k(h_1 + h_2 + h_3)]$ for a three-layered elastic film as a function of $\mu_2/\mu_1 = \mu_3/\mu_2$ for various thickness values $h_2/h_1 = h_3/h_2$ with Poisson's ratios $v_1 = v_2 = v_3 = 0.5$ (open triangles: $h_2/h_1 = h_3/h_2 = 0.1$; open squares: $h_2/h_1 = h_3/h_2 = 1/3$; asterisks: $h_2/h_1 = h_3/h_2 = 1$; open diamonds: $h_2/h_1 = h_3/h_2 = 3$; open circles: $h_2/h_1 = h_3/h_2 = 10$)

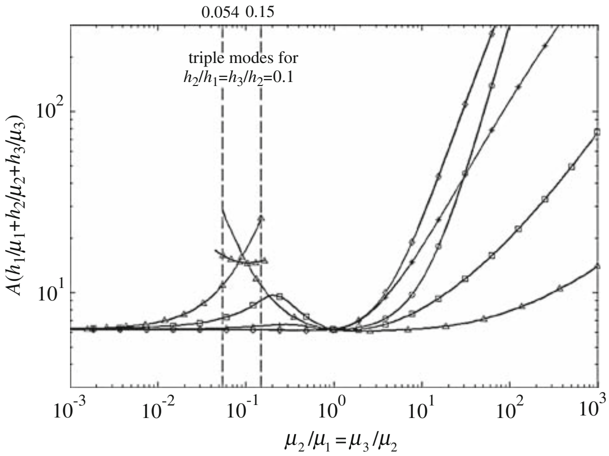

Fig. 9. Dimensionless interaction coefficient $A(h_1/\mu_1+h_2/\mu_2+h_3/\mu_3)$ for a three-layered elastic film as a function of $\mu_2/\mu_1=\mu_3/\mu_2$ for various thickness values $h_2/h_1=h_3/h_2$ with Poisson's ratios $\nu_1=\nu_2=\nu_3=0.5$ (open triangles: $h_2/h_1=h_3/h_2=0.1$; open squares: $h_2/h_1=h_3/h_2=1/3$; asterisks: $h_2/h_1=h_3/h_2=1$; open diamonds: $h_2/h_1=h_3/h_2=3$; open circles: $h_2/h_1=h_3/h_2=10$)

b. A four-layered elastic film interacting with a flat rigid body

Here, we consider the case in which the four layers are compressible with equal Poisson's ration $\nu_1=\nu_2=\nu_3=\nu_4=0.3$. All local minima of A as a function of h_1k are determined. In Figs. 18 and 19, the dimensionless wavelength $2\pi/[k(h_1+h_2+h_3+h_4)]$ and the dimensionless interaction coefficient $A(h_1/\mu_1+h_2/\mu_2+h_3/\mu_3+h_4/\mu_4)$ at all local minima are plotted as a function of the shear modulus ratio $\mu_2/\mu_1=\mu_3/\mu_2=\mu_4/\mu_3$ for h_1:h_2:h_3:$h_4=1$:1/9:1/81:1/729. In this situation four distinct instability modes can exist. The long-wave mode with the dimensionless wavelength $2\pi/[k(h_1+h_2+h_3+h_4)]$ greater than 2.9169 exists when $\mu_2/\mu_1=\mu_3/\mu_2=\mu_4/\mu_3\geq 0.00371$; the short-wave mode with the wavelength smaller than 0.012 exists when $\mu_2/\mu_1=\mu_3/\mu_2=\mu_4/\mu_3\leq 0.00409$; two different intermediate-wave modes with wavelengths between 0.3244 and 0.9098 and between 0.0346 and 0.1051 exist when $0.00319\leq\mu_2/\mu_1=\mu_3/\mu_2=\mu_4/\mu_3\leq 0.00781$ and $0.00179\leq\mu_2/\mu_1=\mu_3/\mu_2=\mu_4/\mu_3\leq 0.00678$.

6.2 Two mutually attracting multilayered elastic films

Here, we examine the surface instability of two mutually attracting multilayered elastic films due to van der Waals forces. The critical value of the interaction coefficient A for the surface instability is

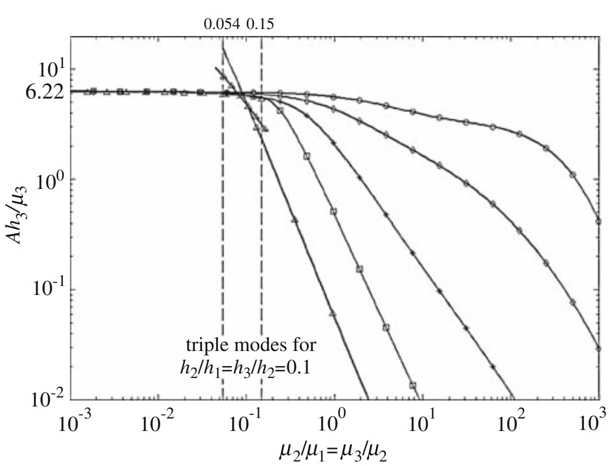

Fig. 10. Dimensionless interaction coefficient Ah_3/μ_3 for a three-layered elastic film as a function of $\mu_2/\mu_1=\mu_3/\mu_2$ for various thickness values $h_2/h_1=h_3/h_2$ with Poisson's ratios $\nu_1=\nu_2=\nu_3=0.5$ (open triangles: $h_2/h_1=h_3/h_2=0.1$; open squares: $h_2/h_1=h_3/h_2=1/3$; asterisks: $h_2/h_1=h_3/h_2=1$; open diamonds: $h_2/h_1=h_3/h_2=3$; open circles: $h_2/h_1=h_3/h_2=10$)

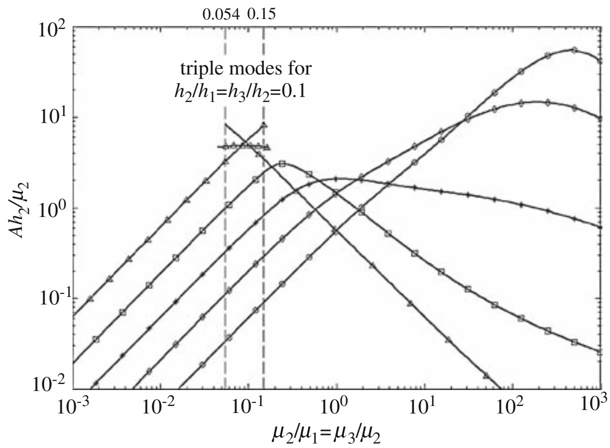

Fig. 11. Dimensionless interaction coefficient Ah_2/μ_2 for a three-layered elastic film as a function of $\mu_2/\mu_1=\mu_3/\mu_2$ for various thickness values $h_2/h_1=h_3/h_2$ with Poisson's ratios $\nu_1=\nu_2=\nu_3=0.5$ (open triangles: $h_2/h_1=h_3/h_2=0.1$; open squares: $h_2/h_1=h_3/h_2=1/3$; asterisks: $h_2/h_1=h_3/h_2=1$; open diamonds: $h_2/h_1=h_3/h_2=3$; open circles: $h_2/h_1=h_3/h_2=10$)

given by the minimum of Eq. (32). We first compare our results with those obtained by Ru [4]; then we present a numerical example for a bilayer elastic film interacting with another single-layer elastic film.

a. Comparison of our results with those of Ru [4]

Due to the fact that our analysis is based on exact elasticity theory for plane strain deformation of the elastic film, while that of Ru [4] is based on an approximate method which reduces a two-dimensional problem of an elastic film to a one-dimensional surface problem, then it is of interest to compare our results with those of Ru [4]. Here we consider the surface instability of two attracting single-layer elastic films due to van der Waals forces. The lower film of thickness h_1 has elastic constants μ_1 and ν_1, while the upper elastic film of thickness h_2 has elastic constants μ_2 and ν_2. We use the definitions $\alpha=h_2/h_1$ and $\beta=(h_2/E_2)/(h_1/E_1)$, where E is the Young's modulus, introduced by Ru [4], Table 1 presents the local minima of Ah_1/E_1 given by Eq. (32) and the corresponding wavenumbers for varying thickness ratio α ($\beta=1$ and $\nu_1=\nu_2=0.5$, and the asterisk indicates the coexistence of two distinct metastable modes; the values in parentheses are those obtained by Ru [4]). The relative errors between our (exact) results and Ru's approximate results are also given. It is found that the accuracy of Ru's results for Ah_1/E_1 is satisfactory with the relative errors less than

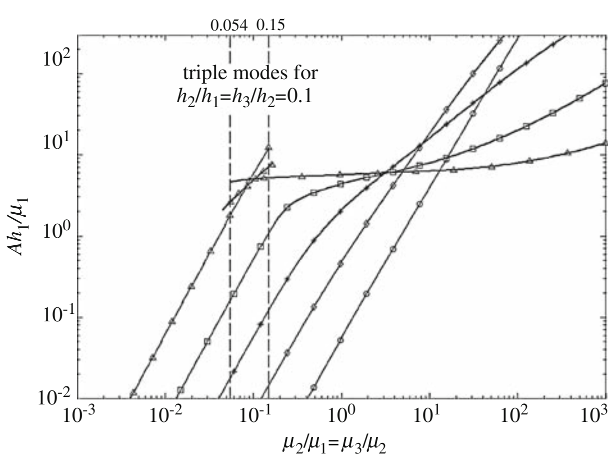

Fig. 12. Dimensionless interaction coefficient Ah_1/μ_1 for a three-layered elastic film as a function of $\mu_2/\mu_1=\mu_3/\mu_2$ for various thickness values $h_2/h_1=h_3/h_2$ with Poisson's ratios $\nu_1=\nu_2=\nu_3=0.5$ (open triangles: $h_2/h_1=h_3/h_2=0.1$; open squares: $h_2/h_1=h_3/h_2=1/3$; asterisks: $h_2/h_1=h_3/h_2=1$; open diamonds: $h_2/h_1=h_3/h_2=3$; open circles: $h_2/h_1=h_3/h_2=10$)

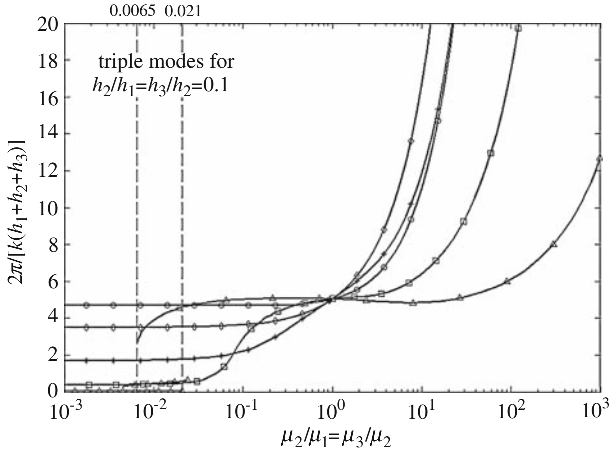

Fig. 13. Dimensionless wavelength $2\pi/[k(h_1+h_2+h_3)]$ for a three-layered elastic film as a function of $\mu_2/\mu_1=\mu_3/\mu_2$ for various thickness values $h_2/h_1=h_3/h_2$ with Poisson's ratios $\nu_1=\nu_2=\nu_3=0.35$ (open triangles: $h_2/h_1=h_3/h_2=0.1$; open squares: $h_2/h_1=h_3/h_2=1/3$; asterisks: $h_2/h_1=h_3/h_2=1$; open diamonds: $h_2/h_1=h_3/h_2=3$; open circles: $h_2/h_1=h_3/h_2=10$)

6%; while the relative errors for $(kh_1)^2$ are considerably large, with the largest relative error at 43.8%. Table 2 gives the local minima of Ah_1/E_1 from Eq. (32) when $\nu_1=\nu_2=0.5$ (for example, ''2.0733 at 4.4944'' means that the value of Ah_1/E_1 is 2.0733 which is attained at $(kh_1)^2=4.4944$; the values in parentheses are those obtained by Ru [4]). One major difference between ours and those of Ru [4] is that our result shows that only one instability mode is found when $\alpha=\beta=100$, while there are two instability modes calculated by Ru [4] for $\alpha=\beta=100$.

b. A bilayer elastic film attracting another single-layer elastic film

Another main discovery of this investigation is that it is possible to find at most N_1+N_2 local minima of metastable instability modes from Eq. (31) for an N_1-layered elastic film interacting with another N_2-layered elastic film. For example, we consider here a lower bilayer elastic film in which the bottom layer has thickness h_1 and elastic constants μ_1, ν_1, and the top layer has thickness h_2 and elastic constants μ_2, ν_2 attracting another upper single-layer elastic film with the thickness h_3 and elastic constants μ_3, ν_3. If we choose $\nu_1=\nu_2=\nu_3=0.5$, μ_1:μ_2:$\mu_3=1$:0.1:10 and h_1:h_2:$h_3=1$:0.1:10, then there exist three local minima in Eq. (32) at $h_1\,k=0.2679$, 1.7074, 16.9543 as shown in Fig. 20.

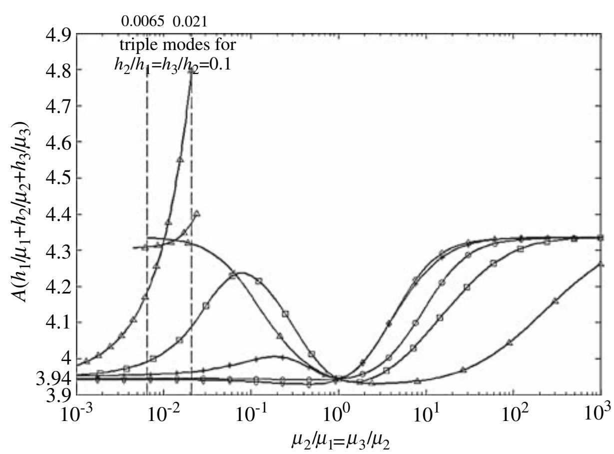

Fig. 14. Dimensionless interaction coefficient $A(h_1/\mu_1+h_2/\mu_2+h_3/\mu_3)$ for a three-layered elastic film as a function of $\mu_2/\mu_1=\mu_3/\mu_2$ for various thickness values $h_2/h_1=h_3/h_2$ with Poisson's ratios $\nu_1=\nu_2=\nu_3=0.35$ (open triangles: $h_2/h_1=h_3/h_2=0.1$; open squares: $h_2/h_1=h_3/h_2=1/3$; asterisks: $h_2/h_1=h_3/h_2=1$; open diamonds: $h_2/h_1=h_3/h_2=3$; open circles: $h_2/h_1=h_3/h_2=10$)

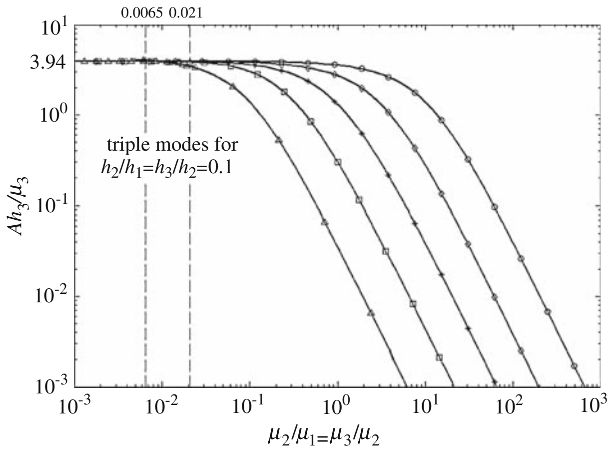

Fig. 15. Dimensionless interaction coefficient Ah_3/μ_3 for a three-layered elastic film as a function of $\mu_2/\mu_1=\mu_3/\mu_2$ for various thickness values $h_2/h_1=h_3/h_2$ with Poisson's ratios $\nu_1=\nu_2=\nu_3=0.35$ (open triangles: $h_2/h_1=h_3/h_2=0.1$; open squares: $h_2/h_1=h_3/h_2=1/3$; asterisks: $h_2/h_1=h_3/h_2=1$; open diamonds: $h_2/h_1=h_3/h_2=3$; open circles: $h_2/h_1=h_3/h_2=10$)

When the upper film is assumed to be a rigid body, then there exist only two instability modes at $h_1 k=1.9953$, 17.3682 as observed by Yoon et al. [6].

6.3 A multilayered elastic film interacting with simply-supported and multilayered elastic plate

We have also recovered the results of Ru [5] for two attracting single-layer elastic films (for example, Figs. 2, 3, 4, 5 in Ru [5]). Here we examine the surface instability of a multilayered elastic film interacting with a simply-supported and multilayered elastic plate through van der Waals forces. The critical value of the interaction coefficient A for the surface instability is given by the minimum of Eq. (36). As an example, we investigate a lower bilayer elastic film in which the bottom layer has thickness h_1 and elastic constants μ_1, ν_1, and the top layer has thickness h_2 and elastic constants μ_2, ν_2 interacting with another upper simply-supported and single-layer elastic plate with thickness h_3, length L and elastic constants μ_3, ν_3. We choose $h_2/h_1=0.1$, $\nu_1=\nu_2=0.5$ and $\mu_2/\mu_1=0.1$ for the bilayer elastic film. Apparently, there are two instability modes when the bilayer elastic film interacts with a rigid body through van der Waals forces. We further choose $\nu_3=0.5$, and assume that the plate is stiffer than both layers of the elastic film. In addition, we introduce the dimensionless parameters $\alpha=h_3/h_1$ and $\beta=(h_3/\mu_3)\ (h_1/\mu_1)$. We plot in Figs. 21, 22

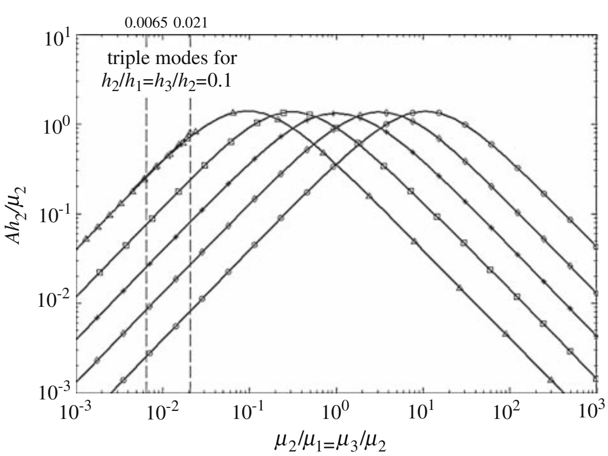

Fig. 16. Dimensionless interaction coefficient Ah_2/μ_2 for a three-layered elastic film as a function of $\mu_2/\mu_1=\mu_3/\mu_2$ for various thickness values $h_2/h_1=h_3/h_2$ with Poisson's ratios $\nu_1=\nu_2=\nu_3=0.35$ (open triangles: $h_2/h_1=h_3/h_2=0.1$; open squares: $h_2/h_1=h_3/h_2=1/3$; asterisks: $h_2/h_1=h_3/h_2=1$; open diamonds: $h_2/h_1=h_3/h_2=3$; open circles: $h_2/h_1=h_3/h_2=10$)

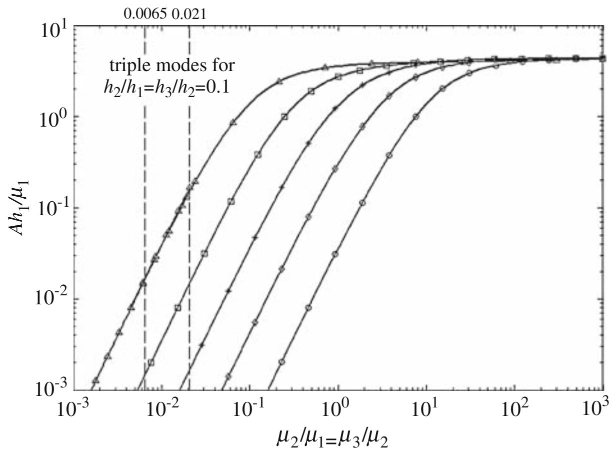

Fig. 17. Dimensionless interaction coefficient Ah_1/μ_1 for a three-layered elastic film as a function of $\mu_2/\mu_1 = \mu_3/\mu_2$ for various thickness values $h_2/h_1 = h_3/h_2$ with Poisson's ratios $\nu_1 = \nu_2 = \nu_3 = 0.35$ (open triangles: $h_2/h_1 = h_3/h_2 = 0.1$; open squares: $h_2/h_1 = h_3/h_2 = 1/3$; asterisks: $h_2/h_1 = h_3/h_2 = 1$; open diamonds: $h_2/h_1 = h_3/h_2 = 3$; open circles: $h_2/h_1 = h_3/h_2 = 10$)

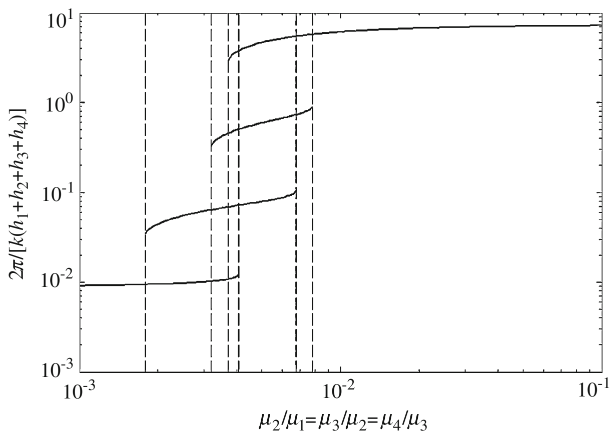

Fig. 18. Dimensionless wavelength $2\pi/[k(h_1 + h_2 + h_3 + h_4)]$ for a four-layered elastic film as a function of $\mu_2/\mu_1 = \mu_3/\mu_2 = \mu_4/\mu_3$ for the thickness value $h_2/h_1 = h_3/h_2 = h_4/h_3 = 1/9$ with Poisson's ratios $\nu_1 = \nu_2 = \nu_3 = \nu_4 = 0.3$

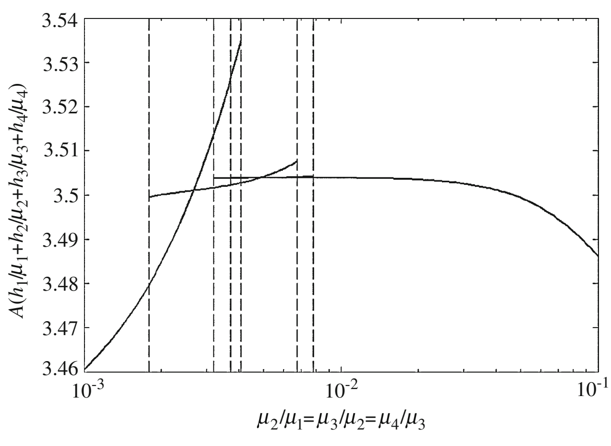

Fig. 19. Dimensionless interaction coefficient $A(h_1/\mu_1 + h_2/\mu_2 + h_3/\mu_3 + h_4/\mu_4)$ for a four-layered elastic film as a function of $\mu_2/\mu_1 = \mu_3/\mu_2 = \mu_4/\mu_3$ for the thickness value $h_2/h_1 = h_3/h_2 = h_4/h_3 = 1/9$ with Poisson's ratios $\nu_1 = \nu_2 = \nu_3 = \nu_4 = 0.3$

and 23 the sixth root of Eq. (36) as a function of $(kh_1)^{1/3}$ for three typical cases $\alpha = 0.05$, $\alpha = 0.5$ and $\alpha = 10$. It is noted that $\alpha = 0.05$ represents the case in which the plate is thinner than each layer of the bilayer film. It is observed from Fig. 21 that, for $\alpha = 0.05$, Eq. (36) has two internal local minima for the smaller values $\beta = 10^{-12}$, 10^{-10}, 10^{-8}; one internal local minimum

Table 1. The local minima of Ah_1/E_1 given by Eq. (32) and the corresponding wave-numbers for two attracting single-layer films under varying thickness ratio α,$\beta = 1$ and $\nu_1 = \nu_2 = 0.5$

α	1.5	3	5	8*		10*		100*		1,000*	
$\frac{Ah_1}{E_1}$	1.0638	1.2405	1.5010	1.7908	1.7268	1.8866	1.7922	2.0701	2.0434	2.0720	2.0733
	(1.1)	(1.21)	(1.44)	(1.75)	(1.81)	(1.86)	(1.9)	(2.06)	(2.06)	(2.063)	(2.063)
	3.4%	2.5%	4.1%	2.3%	4.8%	1.4%	6.0%	0.49%	0.81%	0.43%	0.50%
$(kh_1)^2$	2.8696	1.1524	0.4869	0.1140	2.9929	0.0610	3.3441	4.503×10^{-4}	4.3681	4.490×10^{-6}	4.4944
	(3.0)	(1.4)	(0.7)	(0.15)	(2.15)	(0.075)	(3.35)	(4.75×10^{-4})	(4.75)	(4.8×10^{-6})	(4.8)
	4.5%	21.5%	43.8%	31.6%	28.2%	23.0%	0.18%	5.5%	8.7%	6.9%	6.8%

Asterisk indicates the coexistence of two distinct metastable modes; the values in parentheses are those obtained by Ru [4]

Table 2. The local minima of Ah_1/E_1 given by Eq. (32) when $v_1 = v_2 = 0.5$ (for example, ''2.0733 at 4.4944'' means that the value of Ah_1/E_1 is 2.0733 which is attained at $(kh_1)^2 = 4.4944$)

	$\alpha = 8$	$\alpha = 10$	α=100	$\alpha = 1{,}000$
$\beta = 0.01$			2.0733 at 4.4902 and 167.7768 at 6.8121×10^{-4} (2.05 at 4.8 and 184 at 0.001)	2.0733 at 4.4944 and 184.35 at 4.5029×10^{-6} (2.06 at 4.8 and 206 at 0.0000048)
$\beta = 0.1$	2.0372 at 4.3597 (2.04 at 4.5)	2.0435 at 4.3848 (2.05 at 4.5)	2.0706 at 4.4732 and 20.3021 at 4.6225×10^{-4} (2.06 at 4.8 and 20.5 at 0.0005)	2.0733 at 4.4944 and 20.4894 at 4.4910×10^{-6} (2.06 at 4.8 and 20.6 at 0.000005)
$\beta = 10$	0.2055 at 0.0727 (0.20 at 0.08)	0.2056 at 0.0461 (0.205 at 0.05)	0.2074 at 4.4944×10^{-4} and 1.7922 at 3.3489 (0.206 at 0.00048 and 2.05 at 4.7)	0.2074 at 4.4893×10^{-6} and 2.0733 at 4.4944 (0.21 at 0.000005 and 2.063 at 4.8)
β=100			0.0207 at 4.4944×10^{-4} (0.0206 at 0.00048 and 1.88 at 2.8)	0.0207 at 4.4893×10^{-6} and 2.0733 at 4.4944 (0.021 at 0.000005 and 2.06 at 4.75)

The values in parentheses are those obtained by Ru [4]

corresponding to the mode of the bottom layer of the film disappears and the other one corresponding to the mode of the top layer of the film remains for the intermediate values $\beta = 10^{-6}$, 10^{-4}; both the two internal local minima will disappear for the larger value $\beta = 10^{-2}$. The second case $\alpha = 0.5$ represents the one in which the plate is thinner than the bottom layer of the film but thicker than the top layer of the film. It is observed from Fig. 22 that, for $\alpha = 0.5$, Eq. (36) has two internal local minima for the smaller values $\beta = 10^{-7}$, 10^{-6}, 10^{-5}, 10^{-4}, 10^{-3}; while one internal local minimum corresponding to the mode of the bottom layer of the film will disappear and the other one corresponding to the mode of the top layer of the film still remains for the larger values $\beta = 10^{-2}$, 10^{-1}. Finally, the third case $\alpha = 10$ represents the one in which the plate is thicker than the total thickness of the film. It is observed from Fig. 23 that, for $\alpha = 10$, Eq. (36) always has two internal local minima. In Figs. 21, 22 and 23, when there exist two internal local minimum, the critical value and the instability mode of the film-plate are determined by the smallest of the two internal local minima and the value of Eq. (36) at the admissible lower bound of Eq. (37). When the length L of the plate is sufficiently short, the lower bound of Eq. (37) is so large that the smaller value of the two internal local minima is lower than the value of Eq. (36) at the lower bound. Thus the film-plate system exhibits the instability mode of the film (more

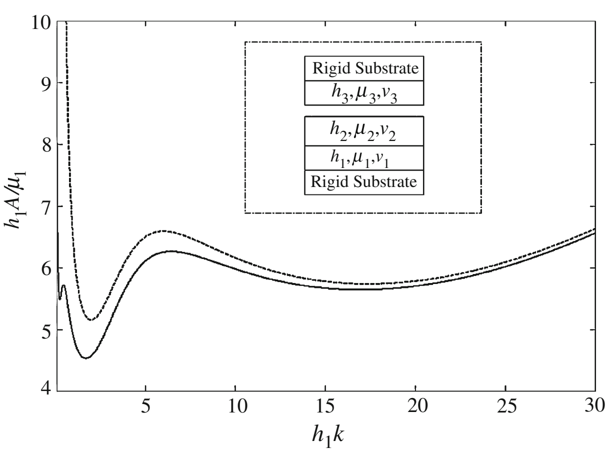

Fig. 20. The interaction coefficient Ah_1/μ_1 in solid lines for a bilayer elastic film interacting with another single-layer elastic film ($v_1 = v_2 = v_3 = 0.5$, $\mu_1{:}\mu_2{:}\mu_3 = 1{:}0.1{:}10$ and $h_1{:}h_2{:}h_3 = 1{:}0.1{:}10$) which, as a function $h_1\ k$, has three local minima (the dashed line is the result when the upper single-layer elastic film is treated as a rigid body)

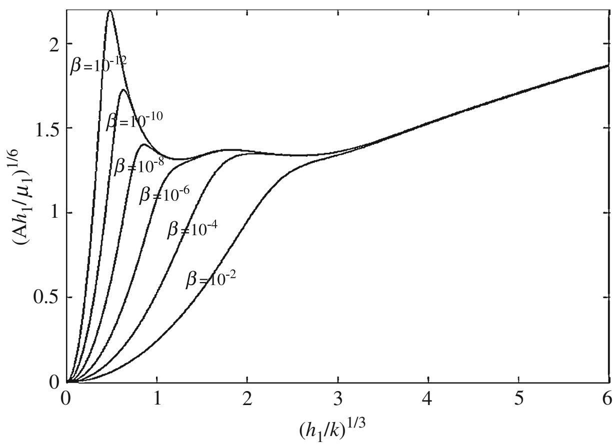

Fig. 21. The interaction coefficient determined by Eq. (36) for a thin plate with $\alpha = 0.05$ which shows the dependency on β of the existence of the internal local minima of Eq. (36)

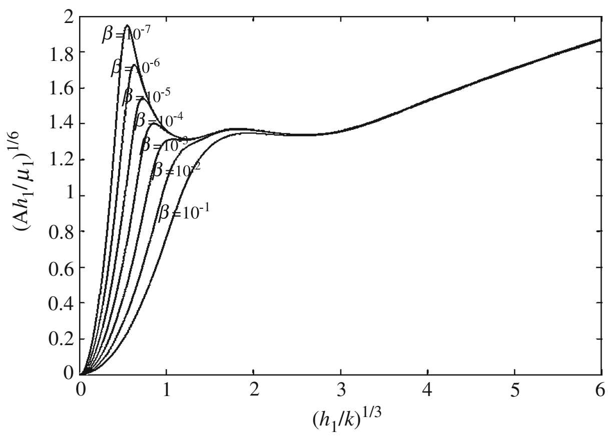

Fig. 22. The interaction coefficient determined by Eq. (36) for a plate of intermediate thickness with $\alpha = 0.5$ which shows the dependency on β of the existence of the internal local minima of Eq. (36)

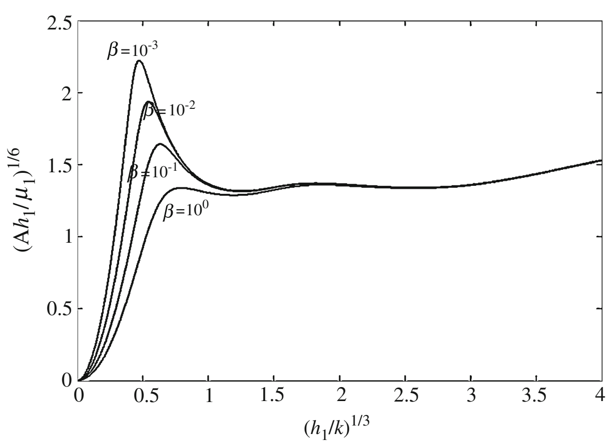

Fig. 23. The interaction coefficient determined by Eq. (36) for a thick plate with $\alpha = 10$ which indicates the existence of two internal local minima of Eq. (36)

specifically, the instability mode of the bottom layer of the film). On the other hand, if the plate is sufficiently long, the lower bound of Eq. (36) is so small that the smaller value of the two internal local minima is still higher than the value of Eq. (36) at the lower bound. In this case the film-plate system exhibits the instability mode of the simply-supported plate. In Figs. 21 and 22, when there exists only one internal local minimum, the critical value and the instability mode of the film-plate are determined by the minor of the internal local minimum and the value of Eq. (36) at the admissible lower bound of Eq. (37). When the length L of the plate is sufficiently short, the lower bound of Eq. (37) is so large that the internal local minimum is lower than the value of Eq. (36) at the lower bound. Thus the film-plate system exhibits the instability mode of the top layer of the film. On the other hand, if the plate is sufficiently long, the lower bound of Eq. (37) is so small that the internal local minimum is still higher than the value of Eq. (36) at the lower bound. In this case the film-plate system exhibits the instability mode of the simply-supported plate. In Fig. 21, when there is no internal local minimum, the film-plate system always exhibits the instability mode of the thin plate, and the two instability modes of the bilayer elastic film will play no role.

7 Conclusions

The pseudo-Stroh formalism and the transfer matrix method are employed here to address three typical kinds of surface instability problems: (1) surface instability of a functionally graded and layered elastic film interacting with another flat rigid body through van der Waals forces; (2) surface instability of two mutually attracting functionally graded and layered elastic films due to van der Waals forces; (3) surface instability of a functionally graded and layered elastic film interacting with another simply-supported functionally graded and layered elastic plate through van der Waals forces. The main results of this research are:

1. It is possible to find N distinct surface instability modes for an N-layered elastic film interacting with another flat rigid body.
2. It is also possible to find at most N_1+N_2 distinct surface instability modes for an N_1-layered elastic film interacting with another N_2-layered elastic film.
3. When a multilayered elastic film interacts with a simply-supported multilayered elastic plate, the film-plate system will exhibit the instability mode of the film or that of the plate depending on the stability strength of the plate versus that of the film.

This research can be considered as an extension of the results in [4]–[6] to the instability of the more general multilayered films or plates, where we adopt a different approach, which is exact in nature, than that in [4]–[6]. Finally, the present formulations can also be easily extended to the case in which each elastic layer is orthotropic [12], and the instability is of three-dimensional nature [7].

Acknowledgements

The reviewers' comments and suggestions were highly appreciated. X.W. and E.P. acknowledge the support from AFRL/ARL. L.J.S. acknowledges the support from the Natural Sciences and Engineering Research Council of Canada through Grant NSERC No. 249516.

References

[1] Monch, W., Herminghaus, S.: Elastic instability of rubber films between solid bodies. Europhys. Lett. **53**, 525–531 (2001)
[2] Shenoy, V., Sharma, A.: Pattern formation in a thin solid film with interactions. Phys. Rev. Lett. **86**, 119–122 (2001)

[3] Shenoy, V., Sharma, A.: Stability of a thin elastic film interacting with a contactor. J. Mech. Phys. Solids **50**, 1155–1173 (2002)
[4] Ru, C.Q.: Surface wrinkling of two mutually attracting elastic thin films due to van der Waals forces. J. Appl. Phys. **90**, 6098–6104 (2001)
[5] Ru, C.Q.: Surface instability of an elastic thin film interacting with a suspended elastic plate. ASME J. Appl. Mech. **69**, 97–103 (2002)
[6] Yoon, J., Ru, C.Q., Mioduchowski, A.: Surface instability of a bilayer elastic film due to surface van der Waals forces. J. Appl. Phys. **98**, 113503 (2005)
[7] Huang, S.Q., Li, Q.Y., Feng, X.Q., Yu, S.W.: Pattern instability of a soft elastic thin film under van der Waals forces. Mech. Mater. **38**, 88–99 (2006)
[8] Ru, C.Q.: Surface instability of a semi-infinite elastic body under surface van der Waals force. ASME J. Appl. Mech. **71**, 138–140 (2004)
[9] Wang, G.F., Schiavone, P., Ru, C.Q.: Surface instability of a semi-infinite harmonic solid under van der Waals attraction. Acta Mech. **180**, 1–10 (2005)
[10] Fried, E., Todres, R.E.: Mind the gap: the shape of the free surface of a rubber-like material in proximity to a rigid contactor. J. Elast. **80**, 97–151 (2005)
[11] Qian, H., Xu, K.Y., Ru, C.Q.: Surface forces driven wrinkling of an elastic half-space coated with a thin stiff surface layer. J. Elast. **86**, 205–219 (2007)
[12] Pan, E.: Exact solutions for functionally graded anisotropic elastic composite laminates. J. Comp. Mater. **37**, 1903–1920 (2003)
[13] Stroh, A.N.: Dislocations and cracks in anisotropic elasticity. Phil. Mag. **3**, 625–646 (1958)
[14] Ting, T.C.T.: Anisotropic Elasticity. Oxford: Oxford University Press 1996
[15] Pan, E.: Exact solutions for simply supported and multilayered magneto-electro-elastic plates. ASME J. Appl. Mech. **68**, 608–618 (2001)
[16] Pan, E., Han, F.: Exact solution for functionally graded and layered magneto-electro-elastic plates. Int. J. Engng. Sci. **43**, 321–339 (2005)
[17] Pan, E.: A general boundary element analysis of 2-D linear fracture mechanics. Int. J. Fract. **88**, 41–59 (1991)